Electric Power Systems Research 122 (2015) 130–139

Contents lists available at ScienceDirect

Electric Power Systems Research

journal homepage: www.elsevier.com/locate/epsr

New ESPRIT-based method for an efficient assessment of waveform distortions in power systems

L. Alfieri [a], G. Carpinelli [a], A. Bracale [b,*]

[a] Department of Electrical Engineering and Information Technology, University of Naples Federico II, Via Claudio 21, Naples, Italy
[b] Department of Engineering, University of Naples Parthenope, Centro Direzionale of Naples, Is C4, Naples, Italy

ARTICLE INFO

Article history:
Received 21 May 2014
Received in revised form 3 January 2015
Accepted 13 January 2015
Available online 30 January 2015

Keywords:
Power quality
ESPRIT method
Parametric methods
Waveform distortions
Spectral analysis

ABSTRACT

Power quality (PQ) is an important issue due to the presence of an increasing number of perturbing and susceptible loads in modern power systems. In this context PQ evaluation requires advanced methods of signal processing that should be accurate and fast. In this paper, a new, advanced, parametric method is proposed that guarantees an accurate estimation of waveform distortions with reduced computational efforts. The method consists of a modified version of the well-known, parametric, high-resolution, sliding window estimation of signal parameters by rotational invariance technique (ESPRIT) method. The main benefit of the proposed scheme is that it significantly reduces the computational effort required to analyze waveforms by evaluating the frequencies and the damping factors of the spectral components one time or, at most, only a few times. Moreover, the waveform was appropriately sampled again to increase the accuracy of the results; the sampling frequency was chosen heuristically using information about the characteristics of the waveform of the power system. Experiments were conducted and the results were compared also in synthesis data. The results showed that the proposed scheme was effective and efficient.

1. Introduction

In a modern power system, power quality (PQ) is an important issue due to the presence of an increasing number of perturbing and susceptible loads linked to the increasing number of dispersed generation units interfaced by converters and large use of non-linear loads [1–3]. Thus, many studies have been performed to characterize and evaluate PQ disturbances [4,5].

In [5], PQ disturbances are classified as "variations" and "events." Variations are (quasi) steady-state disturbances, and events are sudden disturbances with well-defined beginning and ending times. Among variations, distortions of voltage and current waveforms are currently among the most important research topics, due to the widespread use of power electronic converters for supplying loads and interfacing with dispersed generation devices.

As it is well known, static converters generate a wide spectrum of components that can be time varying due to the time variations of their operating conditions.

In order to characterize waveform distortions, international standards and recommendations have proposed indices the calculation of which requires knowledge of the spectral components included in the waveforms that are being studied. The spectral components can have frequencies that are integer or non-integer multiples of the frequency of the power supply, leading to the well-known harmonic and interharmonic components, respectively [6,7]. IEC standards are the most widely applied; they suggest the use of short-term Fourier transform (STFT) to perform spectral analysis over successive rectangular time windows of exactly 10 cycles (for 50-Hz systems) or 12 cycles (for 60-Hz systems) of the waveform fundamental period.

However, STFT can be characterized by reduced accuracy due to the spectral leakage phenomenon caused by [8]:

- errors in synchronizing fundamental frequency and harmonics caused by deviations of fundamental frequency;
- the presence of non-synchronized inter-harmonics.

While the IEC standard is important for quantifying the distortion of the waveform in a reproducible form, it is of limited use for extracting detailed information or for studying individual components.

* Corresponding author. Tel.: +39 0815476757.
E-mail addresses: luisa.alfieri@unina.it (L. Alfieri), guido.carpinelli@unina.it (G. Carpinelli), antonio.bracale@uniparthenope.it (A. Bracale).

http://dx.doi.org/10.1016/j.epsr.2015.01.011
0378-7796/

Several techniques have been proposed in the relevant literature to overcome the shortcomings of the IEC standard [9,10]. In particular, in [10], the most important harmonic estimation techniques were reviewed and classified as (i) non-parametric, (ii) parametric, or (iii) hybrid methods. The non-parametric methods, as is the case for STFT-based methods, provide only a rough estimation of the waveform distortions, and, since their frequency resolutions are fixed, the detection of interharmonics and sub-harmonics is particularly difficult. The parametric methods, e.g., the Prony and ESPRIT methods, were proposed for an accurate assessment of spectral components [11–21]. In the case of the distortion of a time-varying waveform, the sliding window (SW) parametric methods use a window that slides forward successively over time to perform the spectral analysis. In doing so, these methods provide improved estimation of harmonics and interharmonics at the cost of significantly increased computational requirements. In [14,15], modified versions of the Prony's method were proposed to reduce the computational efforts and guarantee acceptable accuracy, but the computational time still exceeded that of the STFT-based methods. In [17], an adaptive algorithm based on the SW ESPRIT method was proposed to estimate the order of the model in each data block and then adjust the size of the autocorrelation matrix. This approach obtained high accuracy and reduced the computational effort, but computational time was still greater than that required by the STFT-based methods. In [19,20], some hybrid methods were proposed in which the SW parametric methods and the STFT-based methods were used together with the aims of providing high accuracy in estimating the spectral components and reducing the computational cost. The computational cost associated with these hybrid methods was significantly less than that of the conventional parametric methods, but it was still significantly greater than that of the traditional, STFT-based methods. Thus, these hybrid methods have two important shortcomings with respect to their detection of the spectral components, i.e., (i) they require the use of a low-pass band filter, which attenuates the amplitude of the low-frequency components and (ii) they may have interharmonics in the waveform analyzed by the synchronized DFT, which, in some cases, could produce residual spectral leakage.

Recently, in [21], another modified version of the Prony's method was proposed. The method proposed in [21] starts from the consideration that the damping factors and the frequencies of the spectral components in power system applications vary slightly with time [9,11–15,19–23] and assumes that the damping factors of the spectral components are equal to zero and that the frequencies are constant and known a priori; this method seems to be particularly interesting because it requires computational effort that is comparable to that required by the traditional STFT-based methods while guaranteeing adequate accuracy in the assessment of the spectral components.

However, the application of the method proposed in [21] requires that the frequencies of all spectral components and the number of components used in the model or the duration of the analysis window must be known a priori; clearly, this is a serious flaw in the method. In addition, Prony's method is known to behave poorly when a signal is corrupted with an added noise.

Motivated by the issues, problems, and requirements indicated above, the aim of the research reported in this paper was to propose a new ESPRIT-based method that guarantees an accurate estimation of waveform distortions and that requires significantly less computational effort than either the traditional parametric methods of the hybrid methods. The computational effort required by the new ESPRIT-based method that we have proposed requires computational effort that is comparable to that required by the traditional STFT-based methods.

As was the case in [21], the method proposed in this paper assumes that the damping factors and the frequencies of all spectral components vary slightly with time, but it also introduces the following substantial improvements:

(i) it is based on the use of the ESPRIT method that is known to behave better than Prony's method when a signal is corrupted by added noise;
(ii) it does not assume that the frequencies of all of the spectral components are known a priori; rather, it calculates the frequencies of the spectral components at least once and, at most, only a few times along the entire signal that is being analyzed;
(iii) it does not assume that the damping factors of all of the spectral components are equal to zero; rather, it calculates the damping factors of the spectral components at least once and, at most, only a few times along the entire signal that is being analyzed.

In addition, it improves the methods in [19,20] by avoiding the use of a low-pass band filter and by avoiding DFT problems caused by residual spectral leakage.

We understand that the proposed approach is not generally applicable, but it is particularly beneficial for many waveforms due to the accuracy of the results and the low computational effort required. Thus, it can be used in practical applications for the rapid and accurate computation of PQ indices [6].

The remainder of the paper is organized as follows. In Section 2, the traditional SW ESPRIT method is described briefly. Section 3 shows the details of the proposed scheme, highlighting the benefits it provides. In Section 4, the results of several experiments are presented, including synthesis and experimental results.

2. Traditional sliding-window ESPRIT method

In this section, we briefly review the traditional sliding-window ESPRIT method for the sake of mathematical convenience in the next section.

The ESPRIT method approximates the waveform samples with a signal model. In particular, for a given sequence of sampled data $x(n)$ of size L, the sampled waveform is approximated by the following linear combination of M complex exponentials [13]:

$$\hat{x}(n) = \sum_{k=1}^{M} A_k e^{j\psi_k} e^{(\alpha_k + j2\pi f_k)nT_s} + r(n), \quad n = 0, 1, \ldots, L-1 \tag{1}$$

where $r(n)$ is the white noise, and A_k, ψ_k, f_k and α_k are the amplitude, initial phase, frequency and damping factor of the kth complex exponential, respectively. Also, they are unknown parameters to be estimated.

Indicating $h_k = A_k e^{j\psi k}$, (1) can be written in a matrix form:

$$\hat{\boldsymbol{x}} = \boldsymbol{V}\boldsymbol{\Phi}^n\boldsymbol{H} + \boldsymbol{r} \tag{2}$$

where

$$\hat{\boldsymbol{x}} = [\hat{x}(n)\ldots\hat{x}(n+N-1)]^T, \quad \boldsymbol{H} = [h_1\ldots h_M]^T$$

$$\boldsymbol{r} = [r(n)\ldots r(n+N-1)]^T$$

$$\boldsymbol{V} = \begin{bmatrix} 1 & 1 & \cdots & 1 \\ e^{(\alpha_1 + j2\pi f_1)T_s} & e^{(\alpha_2 + j2\pi f_2)} & \cdots & e^{(\alpha_M + j2\pi f_M)} \\ \vdots & \vdots & \ddots & \vdots \\ e^{(\alpha_1 + j2\pi f_1)(N-1)T_s} & e^{(\alpha_2 + j2\pi f_2)(N-1)T_s} & \cdots & e^{(\alpha_M + j2\pi f_M)(N-1)T_s} \end{bmatrix}$$

and

$$\boldsymbol{\Phi} = \begin{bmatrix} e^{(\alpha_1+j2\pi f_1)T_s} & 0 & \dots & 0 \\ 0 & e^{(\alpha_2+j2\pi f_2)T_s} & \dots & 0 \\ \vdots & \vdots & \ddots & \vdots \\ 0 & 0 & \dots & e^{(\alpha_M+j2\pi f_M)T_s} \end{bmatrix}$$

is the rotation matrix with $N < L$ the selected order of the correlation matrix.

In this form, the solution of the problem (2) is obtained by using the transformation proprieties of $\boldsymbol{\Phi}$. In particular, the matrix $\hat{\boldsymbol{S}}$ of the eigenvector associated to the first M eigenvalues of the correlation matrix $\boldsymbol{R}_x$, and a matrix $\boldsymbol{\Psi}$ that has the same eigenvalues of $\boldsymbol{\Phi}$ are introduced in order to verify the relation:

$$\hat{\boldsymbol{S}}_2 = \hat{\boldsymbol{S}}_1 \boldsymbol{\Psi} \tag{3}$$

where $\hat{\boldsymbol{S}}_1 = \begin{bmatrix} \boldsymbol{I}_{L-1} & 0 \end{bmatrix} \hat{\boldsymbol{S}}$, $\hat{\boldsymbol{S}}_2 = \begin{bmatrix} 0 & \boldsymbol{I}_{L-1} \end{bmatrix} \hat{\boldsymbol{S}}$ and $\boldsymbol{I}_{L-1}$ is an identity matrix of order $L-1$. In this way an estimation of the matrix $\boldsymbol{\Psi}$ can be achieved by applying the least-squares approach:

$$\hat{\boldsymbol{\Psi}} = (\hat{\boldsymbol{S}}_1^* \hat{\boldsymbol{S}}_1)^{-1} \hat{\boldsymbol{S}}_1^* \hat{\boldsymbol{S}}_2 \tag{4}$$

Computing the eigenvalues $\hat{\lambda}_i$ of the matrix $\boldsymbol{\Psi}$, the element of the main diagonal of $\boldsymbol{\Phi}$ are identified, and, being $\hat{\lambda}_i = e^{\alpha_i + j2\pi f_i}$, the unknown damping factors and frequencies are respectively estimated as real and imaginary part of the natural logarithm of these eigenvalues.

By the knowledge of the damping factors and frequencies, the amplitudes and initial phases are obtained by recurring again to the last-squares approach. Specifically, the amplitudes are evaluated by using the theoretical definition of $\boldsymbol{R}_x$:

$$\boldsymbol{R}_x = \boldsymbol{V}\boldsymbol{A}\boldsymbol{V}^H + \sigma_w^2 \boldsymbol{I} \tag{5}$$

where $\boldsymbol{A}$ is the diagonal matrix of the squares of the unknown amplitudes, $\boldsymbol{I}$ is an identity matrix and σ_w^2 is the variance of the white noise. The initial phases are then estimated by the vector $\boldsymbol{H}$ obtained solving the (2) and imposing that the noise $\boldsymbol{r}$ is negligible.

Note that the complex exponential form in Eq. (1) is equivalent to the exponentially-damped sinusoidal form [13]. Our choice was made only for the sake of clarity, since using the complex exponential form clearly shows the connection between the eigenvalues $\hat{\lambda}_i$ and the unknown frequencies and damping factors in the model (1).

If signal that is being analyzed varies with time, a sliding-window ESPRIT method is required. This is done by using a window that slides forward successively over time, thereby obtaining time-dependent estimates of the spectral components [13,20]. Fig. 1 shows a block diagram of the traditional sliding-window ESPRIT method. Research of the unknown parameters was performed for each selected time window by increasing the M and N values iteratively and solving Eqs. (2) and (5) in order to guarantee a reconstruction error, ε, that was less than the threshold, ε_{th}. It should be noted that great attention must be paid to the choice of the number of exponentials M, the order N of the correlation matrix and the sampling frequency, which are determinants for the accuracy of the results and for the computational effort required [24].

In addition, the value of the error threshold should be fixed on the basis of the accuracy needed in the particular application or it should be a compromise between the computational burden and the required accuracy.

3. New, modified sliding-window ESPRIT method

The sliding-window ESPRIT method provides very accurate results in the spectral analysis of the waveforms of power systems,

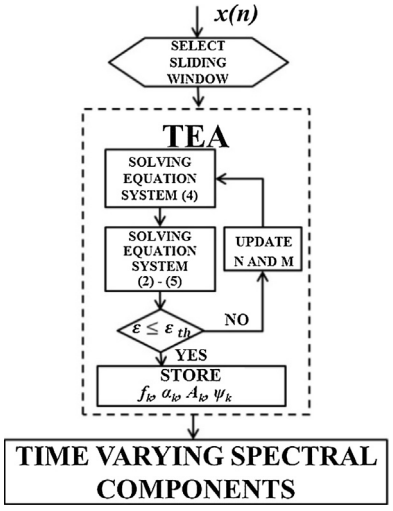

Fig. 1. Traditional, sliding-window, ESPRIT method.

but its computational time is usually very high because Eqs. (4) and (5) must be solved for each window inside the whole signal to be analyzed, and the size of the involved systems can be so large that their solutions become burdensome, depending on the correlation matrix size N (linked to window size L) and the number M of exponentials [13,24].

In this section, we propose a novel scheme that aims at providing accurate estimation of the spectral components of waveforms while keeping the computational cost significantly lower than the efforts required by both the traditional parametric methods and hybrid methods. The proposed scheme modifies ESPRIT's original approach by (i) evaluating the frequencies of the spectral components one time or, at most, only a few times and (ii) evaluating the damping factors of the spectral components one time or, at most, only a few times. Moreover, the waveform is appropriately sampled to increase the accuracy of the results.

In the next sub-sections, these choices are motivated and illustrated with details. The block diagram of the proposed new scheme (Fig. 2) is described and discussed.

3.1. Frequency evaluation

The analysis of time-varying waveforms in several power system applications has shown that in most cases the spectral components of the waveform are characterized by frequencies that are much less variable versus time than amplitudes [11,12,15,19–21].

As an example, Fig. 3a–c shows some spectral components of measured waveforms of a wind-turbine generator during soft starting (Fig. 3a), an arc furnace (Fig. 3b) and a photovoltaic plant (Fig. 3c). As shown in Fig. 3, the main spectral components are harmonics, the frequencies (left column) of which vary slowly with time. This behavior depends mainly on the correlation between the harmonic frequencies and the frequency of the fundamental component, which is slowly and slightly variable with time in modern, interconnected power systems. Also, interharmonic frequencies, if present, vary slowly. We stress that similar behavior is not the general rule, mainly for the frequencies of interharmonics. For example [20,23], adjustable speed drives, cycloconverters or DC arc furnaces can be characterized by interharmonics the frequencies of which are determined by factors that are not correlated with the fundamental frequency, so significant temporal frequency variations can be experienced.

Instead of [21] where the frequencies must be known a priori to apply the proposed method, in this paper we propose to calculate initially the frequencies of the spectral components of

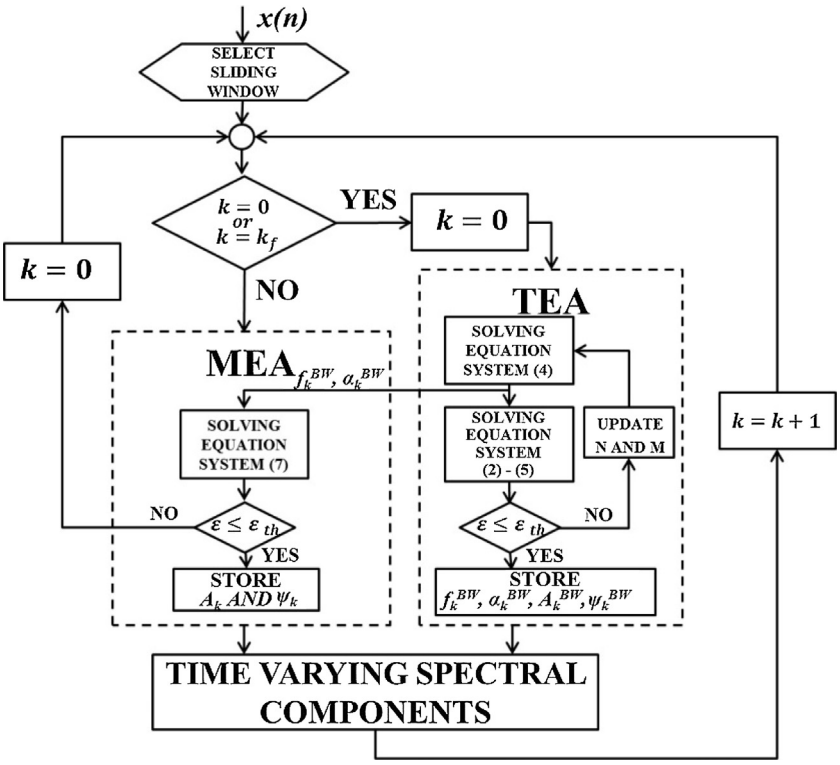

Fig. 2. Block diagram of the new, modified, sliding-window, ESPRIT scheme.

the waveform from the analysis of only the first sliding window, the *basis window*, and we assume that the frequencies in the successive sliding windows, i.e., the *no-basis windows*, were constant.

Moreover, in order to avoid masking effects when frequencies are significantly varying, we propose also to periodically repeat the calculation of frequencies. If the difference between the values calculated in the new basis window and those previously obtained is

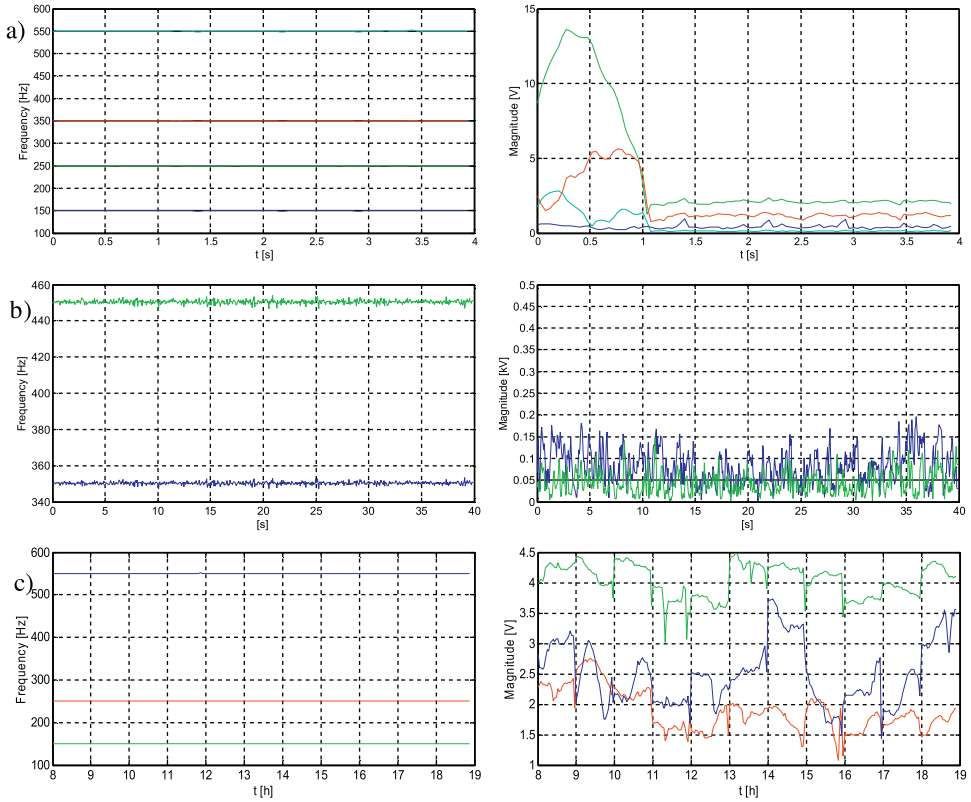

Fig. 3. Frequencies (left column) of the spectral components and amplitudes (right column) of the measured waveforms of a wind-turbine generator during soft starting (Fig. 2a), an arc furnace (Fig. 2b) and a photovoltaic plant (Fig. 2c).

greater than a tolerance value, the frequencies, are updated and the spectral analysis can proceed.

Specifically, as shown in Fig. 2, if k is the window counter with an initial value of 0 and the first analysis window ($k=0$) is a basis window, an integer number k_f is introduced to define the distance between two successive basis windows. The first choice of the value k_f can be determined heuristically based on the knowledge of the waveforms to be analyzed. After the first interval $[0,k_f]$, the choice of the successive values of k_f can be updated using different criteria. For example, k_f could be an integer number that is inversely proportional to the value of the maximum difference between the values of frequencies calculated in the new basis window and those obtained previously. Eventually, with the assumption of constant frequencies inside the no basis windows, we were able to reduce the unknowns to be obtained and the computational effort significantly, as will be described in more detail in the next subsection.

3.2. Damping factor evaluation

Although in the traditional Prony's approach the damping factors have an important role, in [21] they became less significant, because in the case of short duration of the windows, the damping factors usually have very small values (close to zero).

In this paper, instead, since the damping factors contribution to the model grows with increasing of the analysis window duration, we proposed to assume the values of the damping factors of the spectral components inside the *no-basis windows* equal to the values computed in the *basis window*, because a large value of L is required for two reasons:

1. the ESPRIT performance improves with increasing of the order N of the correlation matrix, so, since $N<L$, the value of L has to be a proper number of times the waveform's fundamental period;
2. the ESPRIT algorithm does not require the research of the optimal duration L of the window under examination to improve the estimation of the waveform spectral components, so the L value is constant.

In these circumstances, the aforesaid values of L determine that damping factors cannot be neglected in the ESPRIT model (1), but, since all the windows under examination have the same length, the damping factor values can be assumed almost constant along the windows.

Then, let us assume that the frequencies and damping factors of the exponentials (i) are calculated by applying the traditional ESPRIT method in the basis windows and (ii) are assumed constant along the no-basis windows.

Let us also assume that the amplitudes and initial phases of the exponentials (i) are calculated by applying the traditional ESPRIT method in the basis windows and (ii) are calculated with a new scheme along the no-basis windows.

The required new scheme modifies ESPRIT model (1) in the no-basis windows in such way as:

$$\hat{x}(n)=\sum_{k=1}^{M}A_k e^{j\psi_k}e^{(\hat{\alpha}_k^{BW}+j2\pi\hat{f}_k^{BW})nT_s}+r(n),\quad n=0,1,\ldots,L-1 \tag{6}$$

where the frequencies $\hat{f}_k^{BW}$ and the damping factors $\hat{\alpha}_k^{BW}$ are known from the analysis of the basis windows performed with the traditional ESPRIT method, where the eigenvalue $\hat{\lambda}_k^{BW}=e^{(\hat{\alpha}_k^{BW}+j2\pi\hat{f}_k^{BW})}$ are computed.

With $\hat{\lambda}_k^{BW}$ known, the linear equation system (4) has no longer to be solved, which results in significant reduction of the computational efforts. Only the linear equation system obtained by (5) and (2) must be solved in order to obtain amplitudes and initial phases in the no-basis windows; the result is:

$$\boldsymbol{H}=(\boldsymbol{V}_{BH}^{H}\boldsymbol{V}_{BH}{}^{-1})\boldsymbol{V}_{BH}^{H}\boldsymbol{x} \tag{7}$$

where the meaning of the symbols is obvious.

We show that the order N and the number of exponentials M involved in the analysis of the basis windows also are imposed for the analysis of the no-basis windows, resulting in further improvement in the computational efficiency.

3.3. Resampling

Usually, parametric methods require an adequate sampling rate in order to avoid inaccuracies in the evaluation of the spectral components. These methods, in fact, are able to accurately detect spectral components until a maximum value of frequency that is strictly linked to the sampling rate of the waveform [21,25–27]. Specifically, in [27], it was shown that ESPRIT method is able to detect spectral components with frequencies up to $f_s/2$, where f_s is the sampling rate, but, in some cases the estimation of the components near $f_s/2$ was revealed unstable, so it is recommended to consider the accurately estimated maximum frequency equal to $f_s/4$.

Then, in this paper we selected the sampling frequency heuristically as follows:

- if the characteristics of the waveform being studied are known a priori, the sampling frequency is assumed to be four times the maximum expected frequency of the spectral component; otherwise,
- the sampling frequency is assumed to be four times the maximum frequency of interest.

It should be noted that an inadequate sampling rate produces very high reconstruction errors due to the inability of the method to adequately approximate the waveform. Then, when the reconstruction error is high, the sampling frequency must be increased. It should also be noted that an adequate choice of the sampling frequency allows a faster research of the optimal N and M values, which also contributes to reducing the computational burden.

3.4. Description of the block diagram of the new, modified sliding-window ESPRIT method

Fig. 2 shows the block diagram of the proposed approach.

The first waveform window (*basis window*) is analyzed with the traditional ESPRIT algorithm (TEA), and all of the parameters obtained ($A_k^{BW}, f_k^{BW}, \psi_k^{BW}$) are stored. Then, the no-basis windows are analyzed with the modified ESPRIT algorithm (MEA), in which only the unknown amplitudes A_k and initial phases ψ_k of the spectral components are calculated, solving the equation system (7).

It should be noted that when the number of basis windows increases, the modified ESPRIT method (MEM) approaches the traditional ESPRIT method (TEM) in terms of the accuracy of the results and the computational time.

According to Sections 3.1 and 3.3, in order to improve accuracy: (i) the difference between the frequency values calculated in two successive basis windows (Section 3.1) and (ii) the time domain reconstruction error should be calculated (Section 3.3). In this paper only the time domain reconstruction error is applied since it provides information about both model parameters (i.e., N, M, damping factor and frequencies) variations and adequacy of the chosen sampling frequency.

The time-domain reconstruction error is calculated for each sliding window to ensure that its value is less than a pre-determined threshold (ε_{th}). This control, in the no-basis windows, ensures the

identification of the significant time-variations of the model of the signal determined in the basis window. In other words, the modified ESPRIT algorithm is applied only until the reconstruction error does not exceed the threshold value in the no-basis windows. Note that the reconstruction error check mentioned above is one of the elements that make the proposed method robust and prevents inaccuracies in the model. Another important element that ensures the reliability of the proposed approach is that the value of L is chosen so that it is equal to the number of samples included in a few cycles of the fundamental period (generally four or five cycles). In fact, in such a reduced time interval, the variation of the detected spectral components is expected to be negligible, so the assumption of constant frequency between two consecutive windows becomes more reasonable.

4. Numerical applications

Several numerical experiments were conducted by analysing both synthesized and measured waveforms in order to evaluate the performances of the proposed method. The results of the proposed method (modified ESPRIT method, MEM) also were compared with the results obtained by applying the traditional sliding-window ESPRIT method (TEM), the sliding-window joint ESPRIT-DFT method (JEDM) proposed in [19] (briefly recalled in the Appendix), and the DFT method (DFTM). In all of the numerical experiments, comparisons were made between both the accuracy of the spectral component and computational time.

For the sake of brevity, only four case studies are presented in this section. Specifically, we show the results obtained from the analysis of two test signals and of two measured current and voltage waveforms. The test signals were generated synthetically by making comparisons between the proposed scheme and the other methods using the ground truth values of the spectral components. The measured waveforms are a voltage waveform measured at a low-voltage bus supplying a laser printer and a current waveform of a wind-turbine generator during soft starting.

In particular, case studies 1 and 2 aimed to show the high accuracy of the TEM in the component estimations and the high speed of the DFTM analysis, justifying the choice to use them in subsequent case studies (3 and 4) as references for the other two methods' evaluations in term of results accuracy and computational burden, respectively.

TEM and MEM selected N and M dynamically on the basis of the reconstruction error [14] starting from a duration of 0.02 s. DFTM was applied with window sizes of 10 times the fundamental period, according to the IEC standards. Obviously, for each case study, the results were presented with reference to common durations of the time window so that the methods can be compared easily. Note that, in the case studies related to test signals, the results were obtained by setting a very low threshold value for the reconstruction error for the parametric methods, since we were interested in strongly emphasizing both the maximum allowable precision and the computational time associated with the methods that were used.

MATLAB programs were developed and tested on a Windows PC with an Intel i7-3770 3.4 GHz and 16 GB of RAM.

4.1. Case study 1

The first signal analyzed was a 4 s, acid-test, synthetic waveform that included:

- a fundamental component at 50.03 Hz with an initial amplitude of 100 p.u. that increased by 1.2% for each interval of 0.24 s;
- 3rd, 5th, 7th, 11th, and 13th order harmonics of amplitude, respectively, 3%, 4%, 3%, 1%, and 1% of the fundamental;
- an interharmonic at 86 Hz with an amplitude that was 0.5% of the fundamental.

Table 1
Case study 1: averages errors (%) on amplitudes, frequencies, and initial phases obtained by TEM, JEDM, MEM, and DFTM: (a) fundamental and interharmonic; (b) 3rd, 5th, and 7th harmonics; (c) 11th and 13th harmonics.

(a)

	Average error [%]			
	Amplitude		Frequency	
	Fundamental	Interharmonic	Fundamental	Interharmonic
TEM	4.18×10^{-4}	0.07	4.55×10^{-5}	0.006
JEDM	5.92×10^{-4}	0.06	3.62×10^{-5}	0.005
MEM	1.89×10^{-4}	0.16	8.10×10^{-5}	0.003
DFTM	0.23	12.28	0.06	1.16

(b)

	Average error [%]					
	Amplitude			Frequency		
	3rd	5th	7th	3rd	5th	7th
TEM	0.009	0.008	0.01	3.94×10^{-4}	1.58×10^{-4}	1.76×10^{-4}
JEDM	0.64	0.22	0.19	0.008	0.008	0.008
MEM	0.007	0.004	0.003	3.64×10^{-4}	4.69×10^{-5}	2.01×10^{-5}
DFTM	0.33	0.27	0.38	0.06	0.06	0.06

(c)

	Average error [%]			
	Amplitude		Frequency	
	11th	13th	11th	13th
TEM	0.03	0.03	2.88 × 10−4	2.26 × 10−4
JEDM	0.40	0.34	0.008	0.008
MEM	0.05	0.05	6.49×10^{-5}	3.98×10^{-4}
DFTM	0.50	0.99	0.06	0.06

A white noise, with a standard deviation of 0.001, was added in order to make the waveform more realistic. The sampling rate was 5000 Hz and, for TEM and MEM, reconstruction error thresholds of 10^{-11} were used. TEM, JEDM and MEM were applied to analyze the same number of data blocks and an overlap of 0.04 s was chosen in order to yield smoother results through the windows. JEDM was applied with window sizes of 3 times the fundamental period. Since the waveform varied slowly with time, just one basis window was required for MPM. The percentage errors in the estimates of the spectral components were calculated by using the results obtained from all data blocks and by evaluating their deviation from the actual values.

Table 1 shows the average percentage errors in the amplitudes and frequencies of the spectral components that were obtained by applying all the methods.

From the analysis of the results reported in Table 1, it is evident that TEM and MEM performed similarly and were characterized by errors lower than those for JEDM and DFTM. DFTM furnishes, usually, the higher errors due to the well-known spectral leakage caused by both fundamental desynchronization and presence of interharmonics.

Note that JEDM furnished accurate results for fundamental and interharmonic but, as foreseeable, had spectral leakage problems in the estimation of the harmonic components due to the presence of residual low-frequency interharmonic component in the second step of the method (see Appendix). However, globally, JEDM provided more accurate estimations of all spectral components than DFTM.

Table 2 shows the average computational time of a single data block of 0.2 s analyzed by all of the methods, in per unit of the computational time required by DFTM.

Table 2
Case study 1: average computational time by TEM, JEDM, and MEM in p.u. of time required by DFTM.

	Computational time [p.u.]
TEM	410.2
JEDM	74.4
MEM	10.6
DFTM	1

From the analysis of Table 2, it is evident that using TEM we pay the accuracy with time computation. On the other hand, JEDM furnished acceptable results with a significant reduction of computational burden. Eventually, MEM had a computational time significantly lower than TEM and just one order of magnitude higher than that of DFTM. Thus, the proposed method obtained accuracy as TEM and time computation comparable to DFTM.

We also analyzed the effects of the sinusoidal variation of the fundamental frequency with deviations from 0.01% to 0.1% in the synthetic waveform mentioned earlier. The orders of magnitude of the average percentage errors increased for all of the methods that were used, but, in the comparison of the methods, similar observations were made for the waveform with a constant fundamental frequency. Specifically, when the maximum deviation of frequency was 0.01%, the average percentage errors of MEM have the same orders of magnitude of the average percentage errors of TEM, and they increase by only one order of magnitude with respect to those obtained for the waveform with a constant fundamental frequency (Table 1). When the maximum deviation of frequency was 0.1%, the average percentage errors of the frequencies of TEM and MEM increased by about two orders of magnitude with respect to those obtained for the waveform with a constant fundamental frequency (Table 1). For the estimates of amplitude, the errors of MEM were one order of magnitude greater than those of TEM, and they were two orders of magnitude greater than those presented in Table 1. However, in term of the accuracy of the results, the results provided by MEM approached those provided by TEM better than any other model for every operative condition. With reference to the computational efforts, also in case of the considered variations of fundamental frequency, the methods confirmed the results in Table 2. We repeated the above experiments also increasing the frequency of the sinusoidal variations of the fundamental frequency, with growing errors. Anyway, the calculation of the waveform reconstruction error in each no-basis window helps in the immediate identification of significant time-variations of the signal model. In fact, when the reconstruction error becomes significant, the model is updated, applying the ESPRIT algorithm without assumptions on frequency values in a new basis window. Obviously, the computational efforts grow with the number of basis windows.

4.2. Case study 2

The test waveform was constituted by:

- a fundamental component at 49.98 Hz with an amplitude of 100 p.u.;
- 5th and 7th order harmonic of amplitude that was 2% of the fundamental;
- two interharmonics at 72 Hz and at 423 Hz with amplitudes that were 0.5% of the fundamental and that decreased by 1.1% for each 0.24 s interval.

Once again, a white noise with a standard deviation of 0.01 was added. The sampling rate was 5000 Hz and, for TEM and for the basis window of MEM, reconstruction error thresholds of 10^{-9} were used. Since the waveform varied slowly with time, just one basis window was needed for the MEM. JEDM was applied with window sizes of 5 times the fundamental period. TEM, JEDM, and MEM were used to analyze the same number of data blocks, and an overlap of 0.04 s was chosen in order to yield smoother results through the windows. Table 3 shows the average percentage errors for the fundamental and interharmonics' amplitudes and frequencies. From the analysis of the results provided in Table 3, MEM and TEM provided most accurate and very similar results. It can be noted that TEM and MEM's errors related to the low frequency interharmonic are greater than the ones related to the high frequency interharmonic. This behavior can be explained considering that the low-frequency interharmonic was near to the fundamental frequency leading to the two components interfered with each other. For the high frequency interharmonic, the interference was negligible.

In addition, in some cases, MEM errors are lower than TEM errors; this can be explained observing that, in some windows, TEM's results can be unstable for the high number of variable parameters. On the other hand, the reduced number of variables in non-basis windows of MEM determines a more stable behavior leading to reduced values of errors.

As expected, it clearly appears that DFTM's errors in the estimation of both low and high frequency interharmonics were globally the greatest in term of amplitude and frequency due to the spectral leakage caused by both fundamental desynchronization and the presence of interharmonics.

Eventually, with reference to JEDM results, the fundamental and low-frequency interharmonic errors were about the same order of magnitude of TEM and MEM. Once again, due to spectral leakage, JEDM errors increase for high frequency interharmonic, also if they are lower than DFTM. Table 4 provides the average computational time by all of the methods in per unit of time required by DFTM. Table 4 shows that MEM had a computational time that was about

Table 4
Case study 2: average computational time by TEM, JEDM, and MEM in p.u. of time required by DFTM.

	Computational time [p.u.]
TEM	422
JEDM	80.4
MEM	9.8
DFTM	1

Table 3
Case study 2: averages errors (%) on amplitudes, frequencies, and initial phases obtained by TEM, JEDM, MEM, and DFTM.

	Average error [%]					
	Amplitude			Frequency		
	Fundamental	72 Hz	423 Hz	Fundamental	72 Hz	423 Hz
TEM	0.008	2.31	0.65	0.001	0.16	0.009
JEDM	0.006	1.37	26.14	7.48×10^{-4}	0.14	0.22
MEM	0.008	2.03	0.21	1.94×10^{-4}	5.29×10^{-4}	0.002
DFTM	0.02	21.22	24.57	0.04	2.78	0.47

Table 5
Case study 3: average values of the amplitudes and frequencies of the most significant spectral components detected by TEM, JEDM, and MEM.

	Average value									
	Amplitude [V]					Frequency [Hz]				
	Fundamental	3th	5th	7th	9th	Fundamental	3th	5th	7th	9th
TEM	224.13	2.85	4.94	3.21	1.25	49.96	150.00	250.11	349.89	449.98
JEDM	220.80	3.06	5.04	3.23	1.30	50.00	149.97	249.92	349.94	449.92
MEM	219.92	2.51	5.16	3.33	1.24	49.95	149.16	250.25	349.85	450.34

Table 6
Case study 3: average errors (%) by JEDM and MEM: (a) fundamental and 3rd harmonic; (b) 5th, 7th and 9th harmonics.

(a)	Average error [%]			
	Amplitude		Frequency	
	Fundamental	3rd	Fundamental	3rd
JEDM	1.49	7.37	0.08	0.02
MEM	1.88	11.93	0.02	0.56

(b)	Average error [%]					
	Amplitude			Frequency		
	5th	7th	9th	5th	7th	9th
JEDM	2.02	0.62	4.00	0.08	0.01	0.01
MEM	4.45	3.74	0.8	0.06	0.01	0.08

one order of magnitude less than that JEDM and that was about the same as the time required by DFTM demonstrating the effectiveness of the proposed approach also in presence of fundamental desynchronization and multiple interharmonics.

4.3. Case study 3

A 3 s voltage waveform measured at a low voltage bus supplying a laser printer was analyzed. The sampling rate was 25 kHz, and it was adequate for estimating the low-frequency components until 5 kHz that was the maximum frequency of our interest. TEM, JEDM, and MEM were used to analyze the same number of data blocks with an overlap of 0.025 s. For TPM and for the basis window of MPM, a reconstruction error threshold equal to 10^{-5} was used. JEDM was applied with window sizes of 3 times the fundamental period.

Also in this case study MEM required just one basis window because the waveform varied very slowly with time.

In addition to the fundamental component, many harmonics were detected by all of the methods, the most significant being the 3rd, 5th, 7th, 9th, 11th, 13th, and 15th-order harmonics.

Table 5 shows the average values of the amplitudes and frequencies of the most significant spectral components evaluated by TEM, JEDM, and MEM. In Table 6, for the same components, JEDM's and MEM's average percentage errors for amplitudes and frequencies are shown by comparing them with the results obtained by TEM. In fact, as mentioned before, since the previous two test cases showed that TEM and DFTM globally provided the best estimation of the spectral components and the more reduced time computation, TEM and DFTM were assumed as references for accuracy and time computation, respectively. However, it is fair to say that this case study is particularly comfortable for the DFTM, since in this waveform the significant components are slowly varying harmonics.

From Table 6, it appears that JEDM and MEM provided similar results for all the components in terms of both amplitude and frequency, with percentage errors having the same order of magnitude. This can be explained with the absence of significant high frequency interharmonics in the measured signal. Table 7 compares the average computational time on a single data block analyzed by

Table 7
Case study 3: computational time by TEM, JEDM, and MEM in p.u. of time required by DFTM.

	Computational time [p.u.]
TEM	2918
JEDM	30.36
MEM	4.23
DFTM	1

Table 8
Case study 4: average percentage errors of the most significant spectral components detected by JEDM and MEM.

	Average error [%]					
	Amplitude			Frequency		
	Fundamental	5th	7th	Fundamental	5th	7th
JEDM	2.20	6.77	6.96	0.26	0.27	0.13
MEM	4.11	6.53	12.13	0.50	0.30	0.11

all of the considered methods. Once again, MEM was faster than the other two methods; in addition it worked much better in this case study 3 than in case studies 1 and 2.

4.4. Case study 4

A current waveform measured during the soft starting of an asynchronous generator was analyzed. The duration of the analyzed waveform was about 5 s. The sampling rate was 2048 Hz, so, as discussed in Section 3.1, a resampling was necessary to allow a proper spectral analysis of the TEM and the MEM, so a sampling rate equal to 10 kHz was chosen.

TEM, JEDM, and MEM were used to analyze the same number of data blocks, and an overlap of 0.02 s was chosen. For TEM and for the basis windows of MEM, a reconstruction error threshold of 10^{-7} was used. This is a waveform with a high time-varying nature in the first 2 s, so MEM was set to analyze a basis window whenever the reconstruction error exceeded 10^{-3}.

The most meaningful components detected by all of the methods were the 3rd, 5th, 7th, and 11th-order harmonics, in addition to the fundamental component. Fig. 4 shows the amplitude of the fundamental harmonic (Fig. 4a), the 5th-order harmonic (Fig. 4b), and the 7th-order harmonic (Fig. 4c) obtained by using TEM, JEDM, and MEM. All of the methods were characterized by similar behavior versus time.

Assuming once again the TEM values as the reference, the mean percentage errors in the estimations of the spectral components for JEDM and MEM were calculated, and they are shown in Table 8. MEM and JEDM provided globally the same results in terms of amplitudes and frequencies.

Note that this case study was characterized by an important issue that occurred in some of our applications, i.e., TEM's results furnished spectral components characterized by very low amplitudes that frequently change versus time, in a non-linear behavior. This phenomenon, physically difficult to explain, seems to be linked to numerical problems due to the very low values

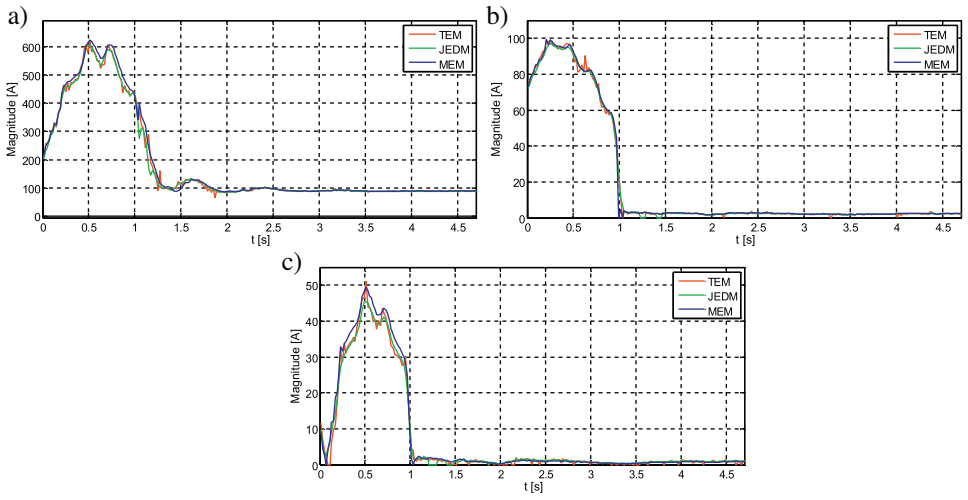

Fig. 4. Case study 4: (a) fundamental, (b) 5th, and (c) 7th-order harmonic components versus time evaluated by TEM, JEDM, and MEM.

Table 9
Case study 4: computational time by TEM, JEDM, and MEM in p.u. of time required by DFTM.

	Computational time [p.u.]
TEM	125.55
JEDM	8.43
MEM	1.60
DFTM	1

of spectral component amplitudes. Then to avoid the possible presence of spurious results, we introduce a threshold value equal to 2% of the fundamental amplitude, below which the components estimated by TEM were not used as references for the estimations of the percentage errors of JEDM and MEM.

It has to be emphasized that JEDM and MEM partially exceeded the above problem that characterizes TEM. In fact, JEDM was always able to detect the low-amplitude harmonic components, since they were evaluated by the DFT algorithm. MEM was able to detect all of the spectral components evaluated in the basis window, even if their amplitudes decreased, since the reduces number of variables in non-basis windows.

Although the DFTM results are omitted in the aforementioned table and figures, it's fair to say that in this case study DFTM has more problems in the components estimation (i.e. the average error on the 7th harmonic amplitude is more than 24%), since the highly time-varying nature of the waveform.

Table 9 shows a comparison of the computational time of a single data block analyzed by all of the considered methods. MEM was faster than the other two methods, and it approached DFTM better than they did; in particular, in this case study MEM approached DFTM much better than in the previous case studies, indicating that MEM is very powerful in the presence of long waveforms, since, in these cases, the computational burden of the basis windows is more mediated.

5. Conclusions

In this paper, we proposed an advanced, new ESPRIT-based scheme for the accurate assessment of waveform distortions in power systems at relatively low computational cost.

The proposed scheme was tested and evaluated on waveform recordings measured in the power system and on synthetically-generated data sequences.

The method was based on the assumptions that the frequencies of the spectral components can be calculated once or, at most, a few times along the analyzed waveform and that the damping factors too can be assumed almost constant along the windows, thereby significantly reducing the computational effort that is required.

Although the proposed approach cannot be considered to be generally applicable, we contend that it is particularly beneficial for many waveforms, in terms of both the accuracy of the results and the reduced computational efforts.

The main outcomes of the scheme were:

(i) Guaranteed a sufficiently accurate estimation of the spectral components for many waveforms, significantly reducing the estimation error.
(ii) Resulted in a significant reduction of the computational time compared to the conventional ESPRIT method without sacrificing the performance of estimation.
(iii) Resulted in a significant reduction of the computational time compared to the recent hybrid ESPRIT-DFT methods, guaranteeing better performance of estimation.
(iv) Resulted in a significant improvement of the accuracy of the results compared to the DFT method, guaranteeing sometimes quite similar and sometimes similar computational time.

Overall, the proposed scheme seems to be a useful method for spectral analysis in terms of both the accuracy of the results and the reduced computational burden, particularly in the presence of waveforms that have frequencies that vary slightly with time.

Appendix A.

A.1. Sliding window joint ESPRIT-DFT method

Sliding window joint ESPRIT-DFT scheme applies either SW ESPRIT method and SW DFT in three different steps, for separately estimating low frequency components (fundamental and interharmonics in a low-pass filtered [0,100]Hz band), harmonics and high frequency interharmonics of power system waveforms [19]. The aim is to reduce the typical problems that generally arise in SW DFT and SW parametric method application, i.e., spectral leakage problems and high computational efforts, respectively.

In the first step, either SW ESPRIT is applied to a low-pass filtered waveform to estimate the power system fundamental and some low frequency interharmonic components. The low-pass band is [0,100]Hz. When SW ESPRIT is applied, then each window of the filtered waveform is approximated with a linear combination of exponentials according to the ESPRIT model (1). The output from

this step includes also the estimated parameters of the fundamental component from which we can calculate the fundamental period. The window size of the SW DFT applied in the second step is set to be an integer-multiple of this estimated fundamental period in order to minimize the spectral leakage.

More in details, by reconstructing the low-pass band components $\hat{\boldsymbol{x}}_{l.f.}(n)$, in the second step the DFT with synchronized window size is applied to the remaining waveform for estimating power system harmonics. The remaining waveform $\boldsymbol{x}_1(n)$ is obtained subtracting the reconstructed waveform $\hat{\boldsymbol{x}}_{l.f.}(n)$ to the starting signal $\boldsymbol{x}(n)$.

According to IEC standard, the time-window size can be set to 10 cycles or 12 cycles of $\hat{T}_{fund}$, respectively, at 50 Hz or 60 Hz. The synchronized window in the DFT application allows to estimate accurately the harmonic component parameters without spectral leakage and with very low computational burden, although the presence of interharmonics in the signal $\boldsymbol{x}_1(n)$ can introduce some spectral leakage that produces errors.

By adding all the reconstructed harmonic components, the waveform $\hat{\boldsymbol{x}}_{harm}(n)$ is obtained and, then, it is subtracted to $\boldsymbol{x}_1(n)$ to obtain the residual $\boldsymbol{x}_2(n)$, that is sent to the third and last step where it is analyzed by ESPRIT method. The residual $\boldsymbol{x}_2(n)$ is usually constituted by a low number of components, which should be all interharmonics in high-pass band (f > 100 Hz).

The reduced number of exponentials in first and third steps guarantees a computational effort lower than applying the SW ESPRIT to the full band signal while the results maintain high accuracy.

Note that the causes of inaccuracies in the estimation of spectral components by the sliding window joint ESPRIT-DFT method are due to: (i) the presence of the low-pass band filter, which introduces a slight attenuation in the estimated low-frequency spectral components; (ii) the presence of interharmonics in the waveform analyzed in the second step by the synchronized DFT, which can introduce spectral leakage problems, which can be particularly significant if the number of those interharmonics increases. The Modified ESPRIT Method proposed in this paper is able to overcome both of these limitations because (i) filter and the amplitude attenuations are absent, since it eliminates the need for any decomposition of the waveform in different frequency bands and (ii) DFT is not used in the proposed method, which eliminates the problems associated with frequency resolution and spectral leakage.

References

[1] F. Blaaiberg, Z. Chen, S. Baekhoej Kjaer, Power electronics as efficient interface in dispersed power generation systems, IEEE Trans. Power Electron. 19 (September (5)) (2004) 1184–1194.

[2] A.R. Di Fazio, G. Fusco, M. Russo, Decentralized control of distributed generation for voltage profile optimization in smart feeders, IEEE Trans. Smart Grid 4 (3) (2013) 1587–1596.

[3] R. Angelino, A. Bracale, G. Carpinelli, M. Mangoni, D. Proto, Dispersed generation units providing system ancillary services in distribution networks by a centralized control, IET Renew. Power Gen. 5 (4) (2011) 311–321.

[4] P. Caramia, G. Carpinelli, P. Verde, Power Quality Indices in Liberalized Market, John Wiley & Sons, Chichester (West Sussex, UK), 2009.

[5] M. Bollen, I. Yu-HuaGu, Signal Processing of Power Quality Disturbances, Wiley-IEEE Press, New Jersey, 2006.

[6] IEC Standard 61000-4-30, Testing and Measurement Techniques – Power Quality Measurement Methods, 2003.

[7] IEC Standard 61000-4-7, General Guide on Harmonics and Interharmonics Measurements, for Power Supply Systems and Equipment Connected Thereto, 2002.

[8] A. Testa, D. Gallo, R. Langella, On the processing of harmonics and interharmonics: using Hanning window in standard framework, IEEE Trans. Power Deliv. 19 (1) (2004) 28–34.

[9] G.W. Chang, C.-I. Chen, Measurement techniques for stationary and time-varying harmonics, in: Proc. of 2010 IEEE PES General Meeting, 2010, pp. 1–5.

[10] S.K. Jain, S.N. Singh, Harmonics estimation in emerging power system: key issues and challenges, Electr. Power Syst. Res. 81 (September (9)) (2011) 1754–1766.

[11] T. Lobos, Z. Leonowicz, J. Rezmer, P. Schegner, High-resolution spectrum estimation methods for signal analysis in power systems, IEEE Trans. Instr. Meas. 55 (February (1)) (2006) 219–225.

[12] A. Bracale, G. Carpinelli, Z. Leonowicz, T. Lobos, J. Rezmer, Measurement of IEC groups and subgroups using advanced spectrum estimation methods, IEEE Trans. Instr. Meas. 57 (4) (2008) 672–681.

[13] I.Y.H. Gu, M.H.J. Bollen, Estimating interharmonics by using sliding-window ESPRIT, IEEE Trans. Power Deliv. 23 (January (1)) (2008) 13–23.

[14] A. Bracale, P. Caramia, G. Carpinelli, Adaptive Prony method for waveform distortion detection in power systems, Int. J. Electr. Power Energy Syst. 29 (June (5)) (2007) 371–379.

[15] C.I. Chen, G.W. Chang, An efficient Prony-based solution procedure for tracking of power system voltage variations, IEEE Trans. Ind. Electron. (2013) 2681–2688.

[16] P. Banerjee, S.C. Srivastava, M. Ramamoorty, Fast estimation of dynamic variations in voltage and current phasor for power system application, in: IEEE PES General Meeting, 21–25 July, 2013, pp. 1–5.

[17] S.K. Jain, S.N. Singh, J.G. Singh, An adaptive time-efficient technique for harmonic estimation of nonstationary signals, IEEE Trans. Ind. Electron. 60 (August (8)) (2013) 3295–3303.

[18] S.K. Jain, S.N. Singh, Fast harmonic estimation of stationary and time-varying signals using EA-AWNN, IEEE Trans. Instrum. Meas. 62 (February (2)) (2013) 335–343.

[19] A. Bracale, G. Carpinelli, I.Y.H. Gu, M.H.J. Bollen, A new joint sliding-window ESPRIT and DFT scheme for waveform distortion assessment in power systems, Electr. Power Syst. Res. 88 (July) (2012) 112–120.

[20] A. Bracale, P. Caramia, G. Carpinelli, A new joint sliding-window Prony and DFT scheme for the calculation of power quality indices in the presence of non-stationary disturbance waveforms, Int. J. Emerg. Electr. Power Syst. 13 (December (5)) (2012).

[21] J. Zygarlicki, M. Zygarlicka, J. Mroczka, K.J. Latawiec, A reduced Prony's method in power-quality analysis—parameters selection, IEEE Trans. Power Deliv. 25 (April (2)) (2010) 979–986.

[22] A. Testa, M.F. Akram, R. Burch, G. Carpinelli, G. Chang, V. Dinavahi, C. Hatziadoniu, W.M. Grady, E. Gunther, M. Halpin, P. Lehn, Y. Liu, R. Langella, M. Lowenstein, A. Medina, T. Ortmeyer, S. Ranade, P. Ribeiro, N. Watson, J. Wikston, W. Xu, Interharmonics: theory and modeling, IEEE Trans. Power Deliv. 22 (4) (2007) 2335–2348.

[23] A. Bracale, P. Caramia, P. Tricoli, F. Scarpa, L. Piegari, A new advanced method for assessment of waveform distortions caused by adjustable speed drives, in: Proc. of the 46th Annual IAS Meeting, Orlando, FL, 9–13 October, 2011.

[24] A. Bracale, P. Caramia, G. Carpinelli, Optimal evaluation of waveform distortion indices with Prony and RootMusic methods, Int. J. Electr. Power Energy Syst. 27 (4) (2007).

[25] P. Stoica, R. Moses, Introduction to Spectral Analysis, Prentice Hall, New Jersey, 1997.

[26] O.Y. Bushuev, O.L. Ibryaeva, Choosing an optimal sampling rate to improve the performance of signal analysis by Prony's method, in: 35th Int. Conf. on Telecom. and Sig. Proc. (TSP), 3–4 July, 2012, pp. 634–638.

[27] L. Alfieri, A. Bracale, P. Caramia, G. Carpinelli, Advanced methods for the assessment of time varying waveform distortions caused by wind turbine systems. Part II. Experimental applications, in: 13th IEEE International Conference on Environment and Electrical Engineering, Wroclaw, Poland, 1–3 November, 2013.